

Experimental Evaluation of the Interaction between Geosynthetic Reinforcements and Hot Mix Asphalt

G. H. Roodi, Ph.D., M.ASCE¹; A. M. Morsy, S.M.ASCE²; and
J. G. Zornberg, Ph.D., P.E., M.ASCE³

¹Dept. of Civil, Architectural, and Environmental Engineering, Univ. of Texas at Austin, 301 E. Dean Keeton St., Austin, TX 78712. E-mail: hroodi@utexas.edu

²Dept. of Civil, Architectural, and Environmental Engineering, Univ. of Texas at Austin, 301 E. Dean Keeton St., Austin, TX 78712. E-mail: amr.morsy@utexas.edu

³Dept. of Civil, Architectural, and Environmental Engineering, Univ. of Texas at Austin, 301 E. Dean Keeton St., Austin, TX 78712. E-mail: zornberg@mail.utexas.edu

Abstract

The advent of interlayer reinforcements with a wide range of stiffness properties has provided the opportunity to produce a specially-designed composite material that can enhance pavement performance in various aspects (e.g., rutting, fatigue cracking, reflective cracking). However, reinforcements may negatively affect the bonding between asphalt layers. The objective of this paper is to evaluate experimentally the interlayer de-bonding effect. In particular, reinforced and unreinforced asphalt specimens were tested in a direct shear test setup and their interlayer bond strength was characterized. The reinforcement inclusions used in the testing program involved synthetic materials made from various polymers, including polyester, polyvinyl alcohol, and glass fiber. Results of the experimental program indicated that the de-bonding effect impacts not only the maximum bond strength, but also the stiffness and the average interlayer shear strain at the maximum bond strength. Moreover, coverage ratio and the thickness of the reinforcement yarns were identified as additional important parameters in characterization of the interlayer de-bonding effect.

INTRODUCTION

Geosynthetics have been used as interlayer reinforcements within or between various structural layers of roadway systems to enhance their performance. For instance, geosynthetics have been used between subgrades and subbase layers to fulfill separation, filtration, reinforcement, drainage, and stiffening functions (Zornberg et al. 2013). Also, geosynthetics have been used within base courses or at the interface between base and subbase layers to stabilize road bases under traffic and environmental loads by fulfilling stiffening function (Roodi 2016; Roodi & Zornberg 2012). Moreover, geosynthetics have also been used within or as the interface layer between hot mix asphalt layers to increase the asphalt fatigue life, mitigate the development of thermal and reflective cracking, enhance pavement rutting resistance, extend the life of an overlay, and enhance overall performance of the pavement.

Inclusion of reinforcements within hot mix asphalt overlays has been developed as a new technique for preventive maintenance treatments. Reinforced overlays have been recognized to be particularly effective in mitigation of reflective cracking. Moreover, reinforcement inclusions

in asphalt layers have been reported to enhance pavement rutting performance by distributing the traffic load over a larger area and increasing the stiffness in the asphalt layer (Brown et al. 1985; Ferrotti et al. 2012; Solaimanian 2013). In spite of the benefits result from the use of reinforcements within asphaltic layers, their inclusion may compromise the bonding between the asphalt layers. This impact, which is referred to as interlayer de-bonding effect, is described as a condition where the adhesion between two adjacent asphalt layers weakens and the two layers eventually become separated under excessive horizontal stresses (Brown et al. 2001; Zamora-Barraza et al. 2010).

While significant research has been conducted to assess the behavior of reinforced asphalt overlays, the de-bonding mechanism due to inclusion of the interlayer reinforcement has not been fully characterized. This paper presents preliminary results of a testing program that aimed at understanding the various parameters that would affect the bonding strength of interlayer reinforced overlays.

BACKGROUND

A wide variety of experiments have been developed to characterize various aspects of bonding strength between two asphaltic layers. Among others, the most common method for laboratory evaluation of interlayer bonding involves experiments that are based on direct shear loading. The direct shear tests, which can be conducted without normal pressure applied on the shear surface (referred to as pure direct shear test) or with the normal pressure, involves imposing a constant shear displacement or shear load across a pre-defined plane (i.e., the interlayer plane) until shear failure is reached.

The most popular types of direct shear interlayer tests include the Leutner shear test (Leutner 1979) (which has been incorporated into the Swiss Standard SN 671961), the Layer-Parallel Direct Shear (LPDS) test (developed by Swiss Federal Laboratories for Materials Science and Technology – EMP), the shearing apparatus developed by the Florida Department of Transportation (FDOT) (Sholar et al. 2002), Nottingham shear box, and the Ancona Shear Testing Research and Analysis (ASTRA) developed at Universita Politecnica delle Marche (Canestrari et al. 2005). Although each test has shown reasonable outcomes, the wide variety of shear mechanisms involved in various tests has made comparison among different test values particularly difficult. Moreover, only a few studies were able to identify a threshold for the bonding strength to minimize, or eliminate, de-bonding effect. Based on statistical analysis of the results of interlayer shear tests conducted in a shear collar device at shear displacement rate of 50 mm/min, West et al. (2005) suggested bond strengths lower than 50 psi (345 kPa) to be considered poor and bond strengths higher than 100 psi (690 kPa) to be considered adequate. However, the actual shear stress at which de-bonding may occur remains unknown.

Previous studies have also identified the most important parameters that impact the bond strength as temperature, gradation and roughness of the surrounding surfaces, normal pressure, tack coat adhesion, and tack coat application rate. Bond strength has been reported to significantly decrease as temperature increases (Sholar et al. 2002; West et al. 2005; Leng et al. 2008) such that at relatively high temperatures the contribution by tack coat adhesion to the bond strength essentially becomes insignificant as compared to the shear resistance provided by layer surface roughness. Other laboratory studies on tack coated surfaces versus uncoated surfaces suggested that the tack coat adhesion is generally smaller than the shear resistance provided by layer surface roughness (Canestrari et al. 2005; Mohammad et al. 2005), especially where

surrounding surfaces are composed of comparatively coarse grain aggregates (Sholar et al. 2002; West et al. 2005). The impact on the bond strength of the tack coat type and application rate has been found to vary from negative, to insensitive, and to positive, based on the asphalt materials and testing conditions (Uzan et al. 1978; Mohammad et al. 2005; Leng et al. 2008). The bond strength has also been found to increase as normal pressure on the shear surface increases (Uzan et al. 1978; West et al. 2005).

The potential de-bonding effect caused by the use of geosynthetic at asphalt interfaces has been studied by testing reinforced-asphalt samples versus unreinforced samples. Experimental studies carried out using various testing devices have reported the occurrence of interlayer de-bonding effect as reinforced asphalt samples generally provided lower interlayer resistance in comparison with the resistance provided by unreinforced samples (Pasquini et al. 2013). However, the parameters affecting the de-bonding effect still remain unclear.

TESTING EQUIPMENT

A large-scale direct shear equipment was used to test asphalt specimens (Figure 1). The equipment has a cylindrical shear mold with interior diameter of 150 mm and depth of 150 mm. The shear mold consisted of two halves each of 75-mm depth allowing samples of up to 150-mm total height to be tested. The equipment has a reaction frame, shown in Figure 1a, to allow normal stress and shear force application. The frame is relatively very stiff such that the machine deflection is minimal during testing.

During testing, the cart is pulled by a large pneumatic actuator, which is 30.5-cm diameter and 12.5-cm stroke. The cart moves on four bearings and two linear guide rails as shown in Figure 1b. Since the bottom half of the shear box is attached to the water reservoir, they move monolithically during the test. The shear box halves slide over each other on two side v-rails. The horizontal pneumatic actuator is operated with pressures up to 1725 kPa and can deliver over 120 kN of horizontal shear force. The equipment is used to conduct displacement-controlled direct shear tests, where the shear force is applied by increasing air pressure to the actuator with an airflow control valve and constant inlet pressure. All tests were conducted at a horizontal displacement rate of 0.5 mm/min.

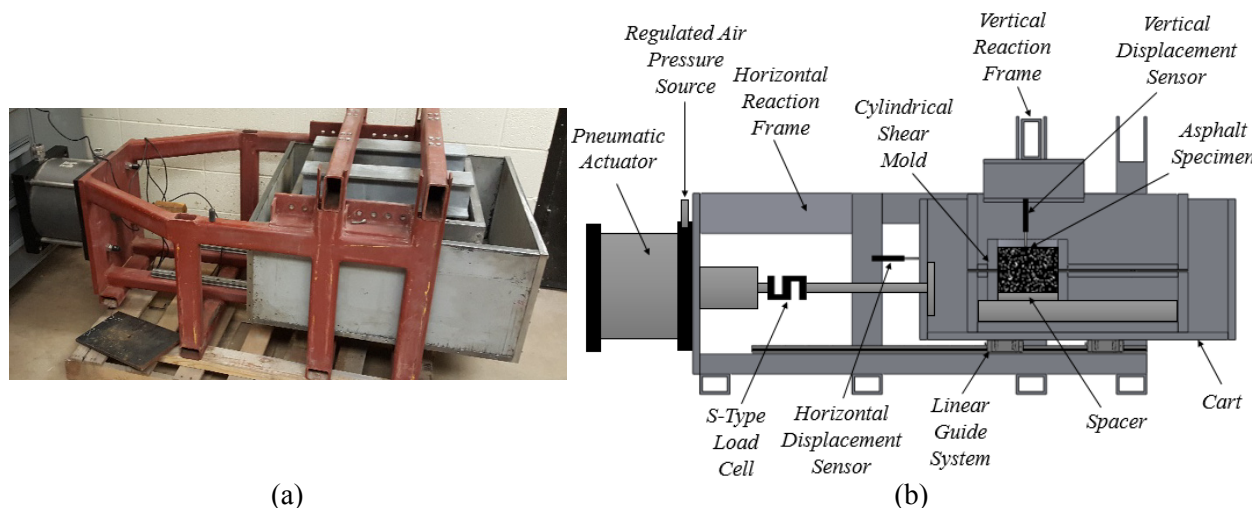


Figure 1. The large-scale direct shear equipment: (a) general view; (b) schematic layout.

The vertical and horizontal displacements of the specimen are monitored by a system of two linear potentiometers: (1) a horizontal potentiometer to measure the relative displacement between the top and bottom boxes; and (2) a vertical potentiometer at the specimen's center. A 10-kip load cell is used to monitor the applied shear force in real-time.

MATERIAL PROPERTIES

The asphalt specimens, made in cylindrical shape, were composed of three primary materials: (1) hot mix asphalt, which were made in two halves: the bottom half represented the old asphalt layer, and the top half represented the new asphalt layer (overlay); (2) emulsifying coat daubed on the top surface of the bottom specimen halves to provide a proper bond with the top specimen halves; and (3) reinforcement materials used at the interface of the bottom and top halves, only in reinforced specimens. The engineering properties of each material are summarized next.

1. Asphalt mix

The hot mix asphalt is composed of two materials: aggregate and asphaltic binder.

1.1. Aggregate

The aggregate used was sieved and re-blended to achieve the desired gradation shown in Figure 2. The coefficient of uniformity (C_u) and coefficient of curvature (C_c) of the blended aggregate were 54.5 and 13.6, respectively. The aggregate was crushed stone with irregular bulky particles having angular edges. The aggregate classifies as A-1-a in accordance to AASHTO M 145 Classification. The weight of aggregate used for one specimen half was 2288 gm (i.e., 4576 gm for one complete specimen). Aggregates of various sizes were blended after the portions from each size were prepared by weight percentage according to the target gradation.

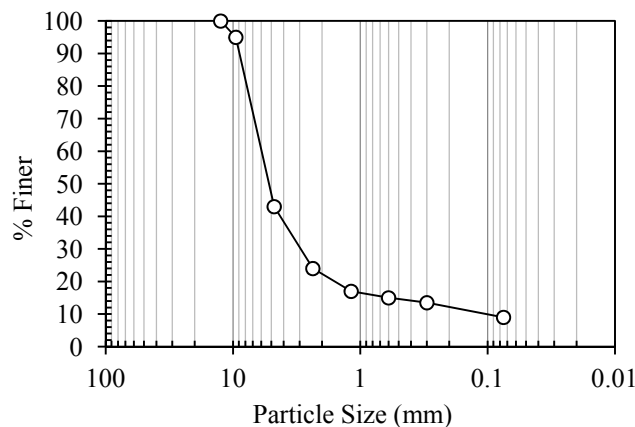


Figure 2. Grain size distribution of the aggregates used in the asphalt specimens.

1.2. Asphaltic binder

The asphaltic binder used in the hot mix asphalt was PG 76-22. The binder was heated before application in the oven at 150 °C for 2 hours until molten. The amount of binder employed for one specimen half was 160 gm (i.e., 320 gm for one complete specimen). This binder consists chiefly of 94-100% asphalt and exists in a semi-solid form. It has melting and boiling points of 43.3-65.6°C and greater than 482.2°C, respectively. The specific gravity of the binder is 0.9-1.1.

2. Emulsifying coat

The emulsifying coat used to bind the new and old asphalt layers was CHFRS-2P. This material is a cationic, high-float, rapid-set emulsion with Butonal NX 1122 polymer. CHFRS-2P was coated on the top surface of the bottom halves of the asphalt specimens. The application was 11 ml +/-9%, which is equivalent to application rate of 0.13 gal/yd² +/-9%. This coat consists chiefly of 50-70% asphalt, 20-40% water, and less than 1% hydrochloric acid. It exists in a liquid form and has melting and boiling points of 65.6-82.2°C and 100°C, respectively. The specific gravity of the coat is 1.03.

3. Asphalt reinforcement

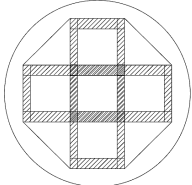
Four different reinforcements were adopted in this study: (1) G1, which is a glass-fiber grid with a 60% bitumen content coating that has tensile strength of 100 kN/m at failure (at 3% strain) in both machine and cross-machine directions; (2) G2, which is also a glass-fiber grid with a 60% bitumen content coating that has tensile strength of 50 kN/m at failure (at 3% strain) in both machine and cross-machine directions; (3) G3, which is a polyvinyl alcohol (PVA) grid with tensile strength of 22 and 50 kN/m at 3% strain and at failure (at 6% strain), respectively, in both machine and cross-machine directions; (4) G4, which is a polyester (PET) grid with tensile strength of 12 and 50 kN/m at 3% strain and at failure (at 12% strain), respectively, in both machine and cross-machine direction. The nominal grid aperture size of G1 and G2 reinforcement is 3 x 3 cm; whereas that of G3 and G4 reinforcements is 4 x 4 cm. All reinforcement types are backed with an ultra-lightweight nonwoven fabric to facilitate field installation. The geometric properties of the various reinforcement types used are summarized in Table 1. Reinforcements were cut to fit in the 150-mm diameter circular cross-section of the asphalt specimens. To maintain the same number of reinforcing elements (longitudinal and transverse ribs) within all reinforced specimens, reinforcements were cut to include 5 apertures as shown in the schematic in Table 2. In addition, Table 2 summarizes the reinforcement coverage ratio in each reinforced specimen. The reinforcement coverage ratio is defined as the ratio of the area covered by the reinforcing elements (reinforcement-asphalt zones) to the total cross-sectional area of the specimen.

Table 1. Reinforcement geometric properties.

Reinforcement Type	Aperture Size (mm x mm) ¹	Longitudinal Rib (Machine Direction)			Transverse Rib (Cross-machine Direction)		
		Yarns Count	Width (mm)	Thickness (mm)	Yarns Count	Width (mm)	Thickness (mm)
G1	28 x 32	2	7	0.8	2	10	1.4
G2	32 x 29	2	6	0.5	2	8.5	0.85
G3	40 x 38	2	3	1.5	6	9	0.8
G4	32 x 38	2	4	2	8	8.5	0.6

¹Aperture size = internal distance between longitudinal ribs (mm) x internal distance between transverse ribs (mm).

Table 2. Interlayer reinforcement coverage ratio.

Reinforcement Type	Reinforcement Coverage Ratio	Schematic
G1	0.276	
G2	0.237	
G3	0.233	
G4	0.215	

TESTING PROGRAM

A series of 5 direct shear tests were conducted on the prepared asphalt specimens including one test on unreinforced (control) specimen and four tests on reinforced specimens. Table 3 summarizes the various configurations of the specimens.

Table 3. Testing matrix.

<i>Test ID</i>	<i>Theme</i>	<i>Emulsifying Coat Weight</i>	<i>Reinforcement Type</i>	<i>Reinforcement Material</i>
U1	Unreinforced	11 ml	N/A	N/A
R1	Reinforced	11 ml below reinforcement	G1	Glass
R2			G2	Glass
R3			G3	PVA
R4			G4	PET

TESTING PROCEDURE

The aggregate and the asphaltic binder were placed in an oven at 150°C for 12 hours and 2 hours, respectively, prior to mixing. The 150-mm diameter compaction mold, mixing paddle, and scoop were also heated in the oven before use. The aggregate was then mixed with the asphaltic binder in the mixing mold using an asphalt mixer. Mixing lasted until the aggregate was fully covered with the binding material, approximately 7 to 10 minutes. The mix was then placed in the oven for 2 hours to age and mixed again for another minute. In preparation of the bottom half of the specimen, the designed amount of the mix was placed in the heated compaction mold and was compacted statically to a height of 57.2 mm. The bottom halves of the specimens, representing the old asphalt layer, were prepared approximately 24 hours before adding the top halves to cool down and 48 hours before testing. The desired amount of emulsifying coat was spread on top of the bottom half and left to dry for 2 hours (Figure 3a). The interlayer reinforcement was then placed on top of the emulsifying coat (Figure 3b) and a light weight was added on top of the reinforcement and left for an hour. The top half was then prepared similarly and compacted on top of the bottom half (Figure 3c). The top halves of the specimens, representing the new asphalt overlay, were prepared approximately 24 hours before testing.

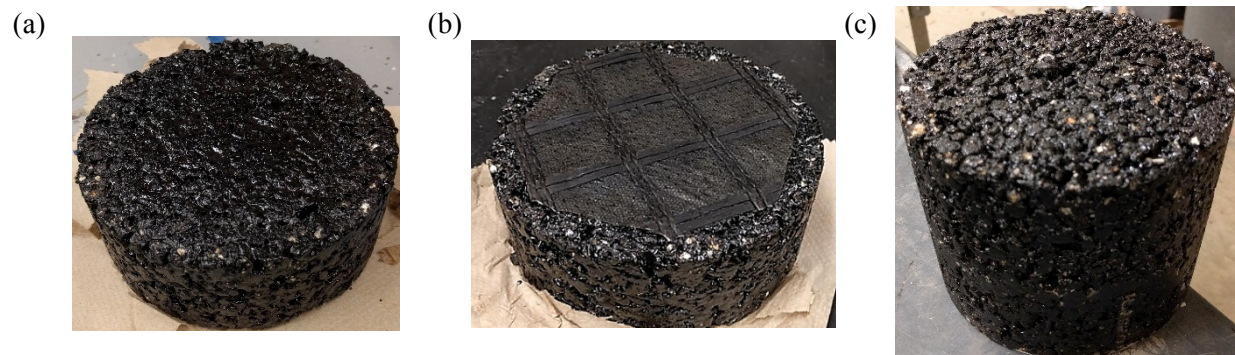


Figure 3. Making asphalt specimens: (a) daubing the emulsifying coat on top of the bottom halves; (b) installing the interlayer reinforcement; (c) completed specimen.

The density and the dimensions (diameter and height) of the specimens were checked prior to testing to affirm compaction quality. The average diameter and height for various specimens ranged from 149.8 mm to 150.1 mm and from 114 mm to 116 mm, respectively. The

average specific gravity and air void of the specimens were also measured as 21.8 kN/m³ and 7%, respectively. The shear tests conducted on the prepared asphalt specimens were displacement-controlled in which the shear displacement rate was 0.5 mm/min. All specimens were tested at zero normal pressure and at temperature of 22.2°C. The two halves of the shear mold were aligned and the specimens were placed such that the interlayer reinforcement, if any, are oriented with their machine direction aligned with the shearing direction.

RESULTS AND ANALYSIS

This section presents the results of the testing program. Specifically, the following subsections presents load-displacement relationship and a brief discussion on interlayer shear surfaces. In addition, a comparison is provided between the bond strength of the reinforced and unreinforced samples, and the samples reinforced with various reinforcement types.

1. Shear load-displacement relationship

Figure 4 presents a typical shear load-displacement relationship obtained in the conducted experiments. This figure illustrates shows the various phases of shear identified in all experiments. The initial segment of the curve (Segment O-A) corresponds to the horizontal load applied to overcome the machine friction and trigger the movement. As the bottom half of the box starts displacing, the horizontal load remains constant (and equal to the machine friction) until the small gaps between the asphalt samples and the mold is covered (Segment A-B). At Point B, the asphalt sample is locked in place and the interlayer shearing starts. Development of shear at the interface continues with a comparatively linear trend until it reaches the maximum bond strength at Point C. The asphalt samples were found to have a brittle failure in which the shear resistance significantly drops after the peak point (Segment C-D). This behavior made capturing the post-peak behavior particularly difficult.

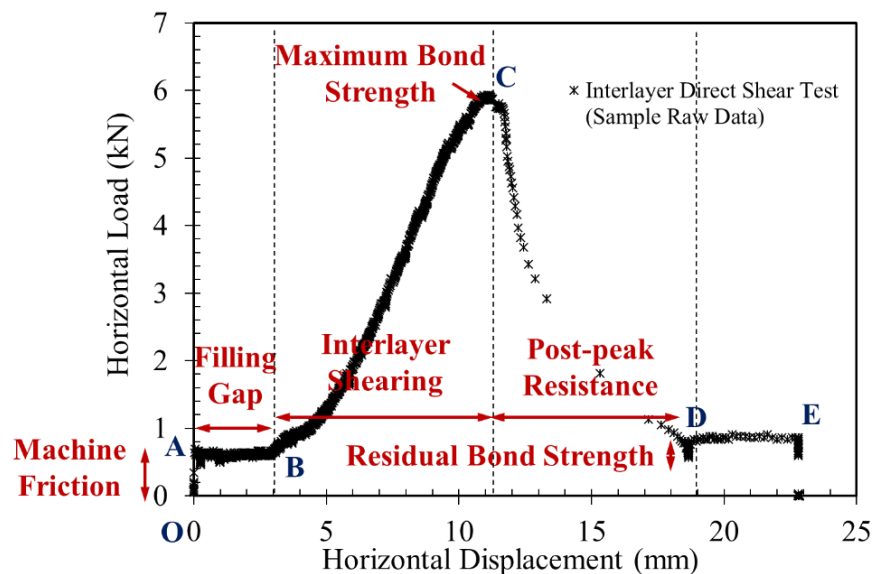


Figure 4. Various phases of interlayer shear test.

The residual shear resistance on the sheared plane was found to be very small. This can be observed from comparing Segment D-E in the curve to Segment A-B. The slight difference in the horizontal load at Segment D-E as compared to that in Segment A-B indicates that the residual shear resistance on the sheared surface is essentially negligible. Consistent with the

focus of this study to evaluate the interlayer shear resistance among different tests, comparison between various tests was carried out based on the shear load-displacement data obtained between Point B (when the interlayer shearing was triggered) and slightly after Point C (the maximum bond strength).

2. Interlayer shear surfaces

As part of the comparison among interlayer shear mechanisms in reinforced versus unreinforced surfaces, the asphalt specimens were forensically investigated after each experiment (Figure 5a). Specifically, the shear surfaces on both halves of the specimens were carefully compared (Figures 5b, 5c, and 5d) and various faces of shear were identified. While in unreinforced specimens the shear load had to overcome the shear resistance between asphalt mix materials, including tack coat, binder and aggregates (Figure 5b), in reinforced specimens the shear plane may pass through three different contact surfaces. Specifically, in a reinforced specimen, three shear resistances may contribute to the overall bond strength: (1) asphalt-asphalt shear, which is relevant to the areas where the asphaltic segments of the top and bottom half-specimens meet (Figure 5d); (2) asphalt-reinforcement shear, which is relevant to the areas where the reinforcement yarns are in contact with asphalt materials (Figure 5c); and (3) inter-reinforcement shear, which is relevant to the shear happens between the filaments of reinforcement yarns (Figure 5d).

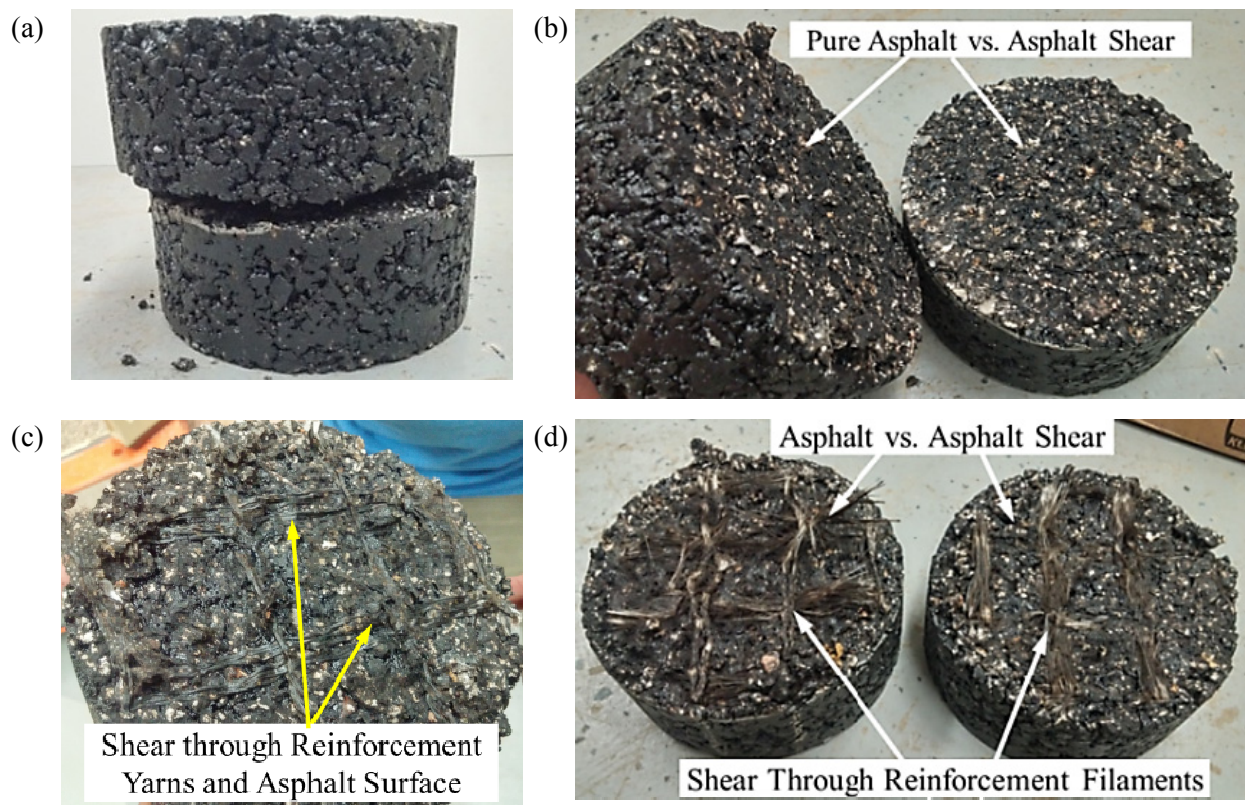


Figure 5. Forensic investigation of the asphalt specimens after shear tests: (a) side view of a sheared specimen; (b) shear plane in an unreinforced specimen; (c) shear plane in a reinforced specimen passing through asphalt-reinforcement yarns interface; (d) shear plane in a reinforced specimen passing through reinforcement filaments.

Understanding the shear behavior between all three surfaces is essential for a full understanding of the interlayer bond strength. Although all three types of shear surfaces were identified in the after-test forensic investigation of the samples, contribution of each type of shear to the overall bond strength and the displacements at which each shear is mobilized are unknown. In particular, characterization of asphalt-reinforcement shear and inter-reinforcement shear, especially based on the polymer type and structural composition of the yarns, might be necessary. Nonetheless, it is often expected that the interlayer shear resistance be compromised by the use of reinforcements between two asphaltic layers.

3. Comparison of the bond strengths of reinforced and unreinforced specimens

The interlayer shear load-displacement relationships for the various specimens are presented in Figure 6. These relationships were reduced from the shear load-displacement data according to the procedure described earlier. The unreinforced sample (U1) were found to provide the highest maximum bond strength as approximately 7.5 kN. The maximum bond strength for the reinforced specimens (R1 through R4) ranged from 4.9 to 6.4 kN, which corresponds to 15 to 35 % decrease compared to the bond strength of the unreinforced specimen. These results indicated that all reinforcements adversely impacted the interlayer bond strength, also known as interlayer de-bonding effect.

While improvement in the performance of reinforced asphalt has been shown to be related to various properties of reinforcement (e.g., mesh size, tensile strength, polymer, coating), the parameters that affects the interlayer bond strength have remained, at best, unclear. In this study, relevant parameters influencing the de-bonding effect was identified as the reinforcement “coverage ratio”, defined as the ratio of the area covered by the reinforcing elements to the total shearing area of the specimen, and the “thickness” of the reinforcement yarns. As the coverage ratio increases, comparatively larger proportion of the asphalt-asphalt shear surface is replaced by asphalt-reinforcement shear surface and correspondingly, the bond strength decreases. Moreover, when thicker reinforcement yarns are used, the contribution of inter-reinforcement shear to the overall bond strength increases, and, considering comparatively lower inter-reinforcement shear resistance, the overall bond strength decreases.

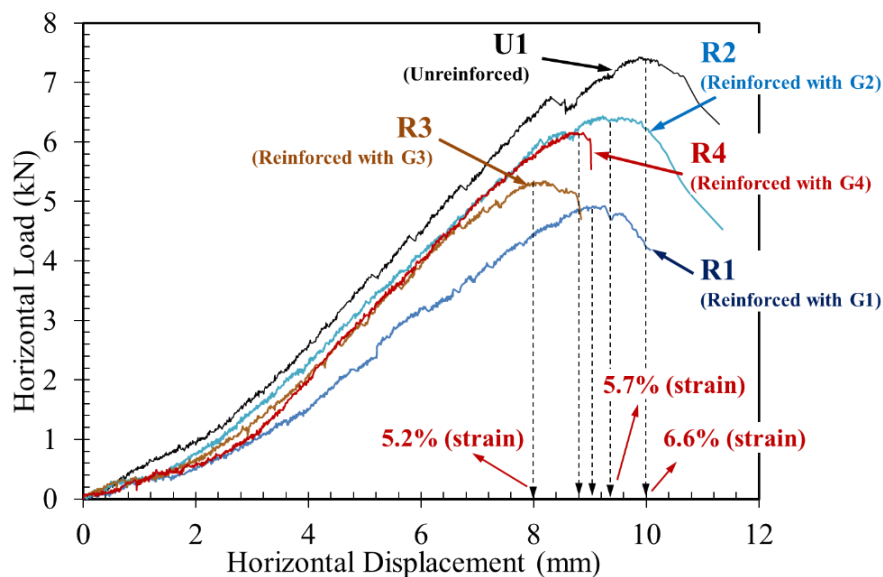


Figure 6. Interlayer shear load-displacement test results

As presented in Table 2, G1 has considerably higher coverage ratio as compared to other reinforcements, which is consistent with the lowest bond strength obtained for specimen R1 as shown in Figure 6. On the other hand, the highest bond strength was found in specimen R2. Although G1 and G2 are made of the same polymer type (glass fibers), the thickness of the yarns in G2 is considerably lower than that in G1. Furthermore, the coverage ratio for G2 is lower than that in G1. Therefore, specimen R2 exhibited comparatively lower de-bonding effect and thus, higher bond strength. In addition, the test conducted on specimen R3 (reinforced with G3) resulted in a lower bond strength than that in specimen R4 (reinforced with G4). The larger bond strength in specimen R4 can also be explained by the difference between the coverage ratio and yarn thickness between reinforcements G3 and G4. Comparison of the rib thicknesses in machine and cross-machine directions presented in Table 1 indicates that the average yarn thickness is almost the same in G3 and G4. However, G3 has comparatively larger coverage ratio than G4 (Table 2), which is consistent with the lower bond strength obtained in specimen R3 than that in specimen R4 (Figure 6).

An additional important finding concerns the slope of the shear load-displacement data, which perhaps correlates with the interface shear stiffness. The slope of the interlayer shear data is expected to be impacted by the slope of the surfaces involved in the shear. The asphalt-asphalt shear provides the highest slope as compared to the asphalt-reinforcement shear and inter-reinforcement shear. This is indeed consistent with the experimental data presented in Figure 6. The slope of the shear load-displacement relationship was found to be the highest when reinforcement inclusions were not used. This slope was anticipated to decrease as the contribution of the reinforcement inclusions in the interlayer shear increases. That is, the same parameters impacting the maximum bond strength (i.e., the coverage ratio and the yarn thickness) are expected to impact the slope of the interlayer shear data. In addition, the slope of the shear load-displacement data was found not to be directly related to the reinforcement polymer type. For example, specimens R1 and R2, both reinforced with glass fiber materials, resulted in significantly different slopes. On the other hand, although reinforced with different polymer types, specimens R2, R3, and R4 showed reasonably similar slopes.

Eventually, evaluation of the experimental data presented in Figure 6 indicates that the interlayer de-bonding effect not only decreases the maximum bond strength of the asphalt layers, but also impacts the shear strain at which the maximum bond strength is realized. As illustrated in Figure 6, inclusion of the reinforcements reduces the average shear strain at the maximum bond strength. The average shear strain, calculated as the ratio of the shear displacement at the maximum bond strength to the specimen diameter (i.e., 150 mm), was found to be about 6.6% for specimen U1, whereas it ranged from 5.2 to 5.7% for reinforced specimens.

CONCLUSIONS

An experimental study was conducted on the mechanisms involved in the interlayer de-bonding effect in reinforced asphalt specimens. Asphalt specimens made with various reinforcement inclusions were sheared using a direct shear test setup at a constant displacement rate of 0.5 mm/min. An unreinforced asphalt specimen was also tested under the same testing conditions. The main findings of the study are as follows: (1) The direct shear device and the testing procedure setup developed as part of this study, were found to be suitable to characterize the interlayer shear properties of reinforced and unreinforced asphalt specimens; (2) The interlayer de-bonding effect was observed for all types of geosynthetic reinforcements used in this study.

The maximum bond strength in reinforced specimens was found to decrease by 15 to 35% compared to corresponding unreinforced specimen; (3) Three shear surfaces were identified to contribute to the mechanisms results in the negative de-bonding effect: asphalt-asphalt shear surface, asphalt-reinforcement shear surface, and inter-reinforcement shear surface. Although all three shear surfaces were identified in the after-test forensic investigation of the sheared specimens, relative contribution of the resistance on each area to the overall bond strength, and the displacements at which each shear mobilizes are unknown; (4) In addition to the polymer type and mass per unit surface of reinforcement, the reinforcement coverage ratio, defined as the ratio of the area covered by the reinforcing elements to the total shearing area of the specimen, and the thickness of the reinforcement yarns were found to be two additional parameters that may impact the interlayer de-bonding effect; (5) The de-bonding effect was found to impact not only the maximum bond strength, but also the slope of the shear load-shear displacement curve and the average shear strain at the maximum bond strength. The slope of the interlayer shear data and the average shear strain at the maximum bond strength were both found to decrease by inclusion of the reinforcements in the asphalt specimens.

REFERENCES

- Brown, S.F., Hughis, D.A.B., Brodrick, B.V. (1985). "Polymer grid reinforcement." *Thomas Telford Limited*, London, 158-165.
- Brown, S.F., Thom, N.H., & Sanders, P.J. (2001). "A study of grid reinforced asphalt to combat reflection cracking." *The Association of Asphalt Paving Technologists*, 70, 543-569.
- Canestrari, F., Ferrotti, G., Partl, M.N., & Santagata, E. (2005). "Advanced testing and characterization of interlayer shear resistance." *TRR*, 1929, 69-78.
- Canestrari, F., Grilli, A., Santagata, F.A., & Virgili, A. (2006). "Interlayer shear effect of geosynthetic reinforcements." *Proc. 10th Inter'l Conf. on Asphalt Pavements*, 811-820.
- Cleveland, G.S., Button, J.W., Lytton, R.L. (2002). *Geosynthetics in flexible and rigid pavements overlay systems to reduce reflection cracking*. Report FHWA/TX-02/1777. TxDOT, Austin, Texas.
- Ferrotti, G., Canestrari, F., Pasquini, E., & Virgili, A. (2012). "Experimental evaluation of the influence of surface coating on fiberglass geogrid performance in asphalt pavements." *Geotextiles and Geomembranes*, 34, 11-18.
- Leng, Z., Al-Qadi, I.L., Ozer, H., & Carpenter, S. (2008). "Tack coat application rate optimization and environmental effect on HMA Overlay-PCC pavement bonding." *Proc. ISAP*, Zurich, Switzerland, 825-835.
- Leutner, R. (1979). "Untersuchung des Schichtverbundes beim bituminösen Oberbau." *Bitumen3*. Hamburg, Germany. (In German).
- Mohammad, L.N., Zhong, W., & Raqib, M.A. (2005). *Investigation of the behavior of asphalt tack interface layer*. Report FHWA/LA.04/394, LTRC, Baton Rouge, Louisiana.
- Pasquini, E., Bocci, M., Ferrotti, G., & Canestrari, F. (2013). "Laboratory characterisation and field validation of geogrid-reinforced asphalt pavements." *Road Mat. & Pav. Design*, 14(1), 17-35.
- Roodi, G.H. (2016). *Analytical, experimental, and field evaluations of soil-geosynthetic interaction under small displacements*. Ph.D. dissertation, Univ. of Texas at Austin.
- Roodi, G.H. & Zornberg, J.G. (2012). "Effect of Geosynthetic Reinforcements on Mitigation of Environmentally Induced Cracks in Pavements." *Proc. of EuroGeo5*, 611-616.

- Sholar, G.A., Page, G.C., Musselman, J.A., Upshaw, P.B., & Moseley, H.L. (2002). *Preliminary Investigation of a Test Method to Evaluate Bond Strength of Bituminous Tack Coats*. Report FL/DOT/SMO/02-459. FDOT, Gainesville, Florida.
- Sobhan, K. & Tandon, V. (2008). "Mitigating reflection cracking in asphalt overlay using geosynthetic reinforcements." *Road Materials and Pavement Design*, 9(3), 367-387.
- Solaimanian, M. 2013. *Evaluating resistance of hot mix asphalt to reflective cracking using geocomposites*. Report No. PSU-2008-04. Pennsylvania State Univ.
- Uzan, J., Livneh, M., & Eshed, Y. (1978). "Investigation of adhesion properties between asphaltic-concrete layers." *Proc. Assoc. of Asphalt Paving Technologists Technical Sessions*, 47, 495-521.
- West, R.C., Zhang, J., & Moore, J. (2005). *Evaluation of bond strength between pavement layers*. NCAT Report 05-08. National Center for Asphalt Technology, Auburn, AL.
- Zamora-Barraza, D., Caldaza-Perez, M., Castro-Fresno, D., & Vega-Zamanillo, A. (2010). "New procedure for measuring adherence between a geosynthetic material and a bituminous mixture." *Geotextiles and Geomembranes*, 28(5), 483-489.
- Zornberg, J.G., Odgers, B., Roodi, G.H., & Azevedo, M.M. (2013). "Advantages and applications of enhanced lateral drainage in pavement systems." *Proc. GeoAfrica*, 539-548.